

Quantum State Tuning of Energy Transfer in a Correlated Environment

Francesca Fassioli,[†] Ahsan Nazir,[‡] and Alexandra Olaya-Castro^{*,‡}

*Department of Physics, University of Oxford, Clarendon Laboratory, Parks Road, Oxford OX1
3PU, UK, and Department of Physics and Astronomy, University College London, Gower Street,
London WC1E 6BT, UK*

E-mail: a.olaya@ucl.ac.uk

Abstract

We investigate multichromophoric energy transfer allowing for bath-induced fluctuations at different sites to be correlated. As a prototype system we consider a light-harvesting antenna surrounding a reaction center. We show that the interplay between quantum coherence and correlated fluctuations can generate a room temperature transfer process featuring a marked dependence on the degree of symmetry and delocalization of the initial exciton state. Our work illustrates how these quantum features could support fine tuning of energy transfer efficiencies in closely-packed natural and artificial light-harvesting complexes.

*To whom correspondence should be addressed

[†]Department of Physics, University of Oxford, Clarendon Laboratory, Parks Road, Oxford OX1 3PU, UK

[‡]Department of Physics and Astronomy, University College London, Gower Street, London WC1E 6BT, UK

Keywords: Quantum yield, quantum coherence, resonance energy transfer, spatial correlations, light-harvesting

Remarkable experimental advances in multichromophoric assemblies have raised the fascinating possibility that quantum coherent dynamics may be relevant in photosynthetic energy transfer, even at room temperature.¹⁻⁵ Key to the survival of quantum coherence in this temperature regime seems to be the emergence of correlated energetic fluctuations between different chromophores.⁶ This could be due, for instance, to closely spaced pigments sharing the same environmental modes.^{2,3} There is thus a growing need for theoretical descriptions of energy transfer beyond the common assumption of independent environments for each pigment.^{7,8} Indeed, a number of studies have addressed this issue,^{6,9-14} though the subtle interplay between coherence and correlated fluctuations in influencing transfer efficiencies remains largely unexplored.

The prospect of environment-protected, room-temperature quantum coherence in photosynthetic systems has revived the longstanding question on the functional role such quantum phenomena may play. In particular, it is natural to ask whether the interplay between coherence and correlated fluctuations provides the system with an *efficiency control mechanism* that it could not otherwise achieve.¹⁵ In this work, we address this question with the aid of a model of multichromophoric energy transfer under the influence of spatially correlated energetic fluctuations. We show that a fundamental signature of the interplay between coherence and correlations is a quantum yield with a conspicuous dependence on the phase information embedded in the initial exciton state. In particular, the energy transfer efficiency can distinguish the degree of symmetry or asymmetry of the initial exciton state, as well as its delocalization length. Such a dependence produces an ordering of the excitonic eigenstates from higher to lower efficiency as a function of increasing energy, a feature which does not exist under local environments. Hence, coherence and correlations can indeed equip large, densely packed photosynthetic systems with a unique mechanism to control their transfer efficiency.

As a prototype system we consider a light-harvesting 1 (LH1) antenna connected to a reaction

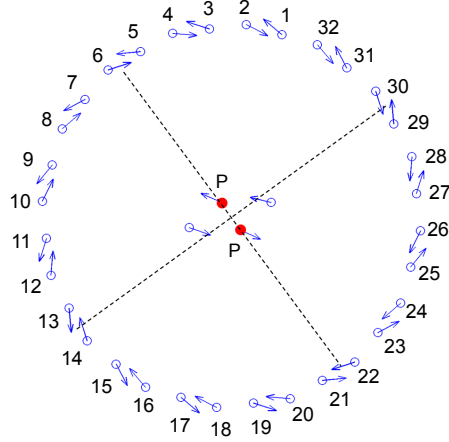


Figure 1: Schematic of the LH1-RC core of purple bacteria based on Ref.¹⁶ Arrows indicate the transition dipole moments for each bacteriochlorophyll (Bchl), as given in Ref.¹⁷ The special acceptor pair in the center (red dots) defines a set of preferred axes of symmetry for the electronic couplings between the center and the LH1 Bchls.¹⁸

center (RC) as in purple bacteria^{16–20} (see [figure][1][1]). We focus on this unit as it exhibits key features, such as symmetry in its geometry and interactions, representative of LH units present in a large variety of natural species²¹ and artificial systems;²² such symmetries are expected to play an important role in the energy transfer process. Evidence of coherence in the LH1-RC core is sparse, though its excitonic states can be delocalized over a large number of pigments at low temperatures.²³ Moreover, it has been shown that correlated energy fluctuations among several Bchls in the LH1 ring must be included to accurately reproduce spectroscopic properties,²⁴ pointing again to the importance of environmental correlations in these densely-packed pigment-protein aggregates. The Hamiltonian describing the electronic excited states of the M strongly interacting pigments of the LH1-RC core is given by $H_S = \sum_{m=1}^M (E_m + \delta E_m) \sigma_m^+ \sigma_m^- + \sum_{n>m} V_{mn} (\sigma_m^+ \sigma_n^- + \sigma_n^+ \sigma_m^-)$, with $\hbar = 1$. The operator σ_m^+ creates a localized excitation at site m , with an energy separated into an ensemble average E_m , and a deviation δE_m that accounts for diagonal static disorder (see supporting information). On-site energies E_m and electronic couplings V_{mn} have been derived from Refs.^{16,17} and they reproduce the observed exciton spectra.²⁵ In contrast to the common assumption of local, independent environmental modes in contact with each pigment, we consider here a single thermal bath described by $H_B = \sum_{\mathbf{k}} \omega_{\mathbf{k}} b_{\mathbf{k}}^\dagger b_{\mathbf{k}}$, where $b_{\mathbf{k}}^\dagger$ ($b_{\mathbf{k}}$) are the creation (annihilation) operators of bosonic modes of frequency $\omega_{\mathbf{k}}$. Each pigment is assumed to have a *position dependent*

coupling to the bath of the form $(g_m)_{\mathbf{k}} = |(g_m)_{\mathbf{k}}|e^{i\mathbf{k}\cdot\mathbf{r}_m}$, with \mathbf{r}_m the position of site m with respect to each phonon mode.²⁶ This position dependence will give rise to correlated energy fluctuations. For simplicity, we consider isotropic and identical coupling strengths for all sites, $|(g_m)_{\mathbf{k}}| \equiv |g_{\mathbf{k}}|$, with associated single-site spectral density $\mathcal{J}(\omega) = \sum_{\mathbf{k}} |g_{\mathbf{k}}|^2 \delta(\omega - \omega_{\mathbf{k}})$, and reorganization energy $E_R = \int_0^\infty d\omega \mathcal{J}(\omega)/\omega$, quantifying the form and strength of the system-bath coupling, respectively. Hence, the system-bath Hamiltonian reads $H_{SB} = \sum_{m=1}^M \sigma_m^+ \sigma_m^- \otimes B_m(\mathbf{r}_m)$, with bath operators written in the interaction picture as $B_m(\mathbf{r}_m, t) = \sum_{\mathbf{k}} |g_{\mathbf{k}}| \left(b_{\mathbf{k}}^\dagger e^{i(\omega_{\mathbf{k}}t + \mathbf{k}\cdot\mathbf{r}_m)} + b_{\mathbf{k}} e^{-i(\omega_{\mathbf{k}}t + \mathbf{k}\cdot\mathbf{r}_m)} \right)$.

Here we consider the limit of weak system-bath interaction for which the energy transfer dynamics can be described with a master equation derived within the Born-Markov and rotating-wave approximations:^{27,28} $\dot{\rho} = -i[H_S + H_{LS}, \rho] + \mathcal{D}(\rho)$. Here, ρ is the reduced system density operator while H_{LS} is the Lamb-shift, which will be neglected. The dissipator, $\mathcal{D}(\rho) = \sum_{\omega} \sum_{m,n} \gamma_{mn}(\omega, d_{mn}) \mathcal{F}_{mn}(\omega, \rho)$, accounts for the effects of both local and correlated fluctuations on the system. The operator $\mathcal{F}_{mn}(\omega, \rho) = A_n(\omega)\rho A_m^\dagger(\omega) - \frac{1}{2}\{A_m^\dagger(\omega)A_n(\omega), \rho\}$, is written in terms of Lindblad operators $A_m(\omega)$, with $\{\omega\}$ the frequency spectrum given by the energy differences between single-excitation eigenstates of H_S . The rates $\gamma_{mn}(\omega, d_{mn}) = \int_{-\infty}^\infty dt e^{i\omega t} C_{mn}(t, d_{mn})$, where $d_{mn} = |\mathbf{r}_m - \mathbf{r}_n|$ is the separation of sites m and n , are defined in terms of bath correlation functions $C_{mn}(t, d_{mn}) = \langle B_m(\mathbf{r}_m, t) B_n(\mathbf{r}_n, 0) \rangle_B$, with the average taken over the thermal equilibrium state of the bath. Evaluating the correlation functions, we obtain a formula relating the spatially-correlated dephasing rates to the on-site rates, $\gamma_{mn}(\omega, d_{mn}) = \mathcal{G}(k(\omega)d_{mn})\gamma_{mm}(\omega)$, where the single-site rate is $\gamma_{mm}(\omega) = \gamma(\omega) = 2\pi \mathcal{J}(|\omega|) |N(-\omega)|$, with $N(\omega)$ being the thermal occupation number. The function $\mathcal{G}(z)$ depends on the environment dimension, exhibiting similar decaying behaviors in two and three dimensions.²⁶ Here, we assume a two-dimensional bath such that $\mathcal{G}(z) = J_0(z)$, with $J_0(z)$ being a Bessel function of the first kind. The function $k(\omega)$ defines an effective bath correlation length, which as a first approximation we assume to have a frequency-independent form $k(\omega) = 1/R_B$, accounting for a phenomenological correlation length R_B .⁹ We can now simplify the dissipator as $\mathcal{D}(\rho) = \sum_{\omega} \gamma(\omega) [\sum_m \mathcal{F}_{mm}(\omega, \rho) + \sum_{n \neq m} J_0(d_{mn}/R_B) \mathcal{F}_{mn}(\omega, \rho)]$, where the first term accounts for independent, on-site fluctuations,

and the second for correlated processes. Using the property $\sum_{m,n} \mathcal{F}_{mn}(\omega, \rho) = 0$, we can demonstrate that for $R_B \rightarrow \infty$, we have $\mathcal{D}(\rho) \rightarrow 0$. In this limit all sites are fully correlated, and the single-excitation subspace of H_S is effectively decoupled from the bath. In the opposite limit of vanishing R_B , we recover the case that each site experiences only local fluctuations, $\mathcal{D}(\rho) = \sum_{\omega,m} \gamma(\omega) \mathcal{F}_{mm}(\omega, \rho)$.

Over the course of the system's evolution any initial excitation will eventually be either dissipated or trapped, with respective rates Γ_m and κ_m for each site. These two incoherent processes can be accounted for by the inclusion of a non-hermitian operator, $H_{\text{proj}} = -i \sum_m (\Gamma_m + \kappa_m) \sigma_m^{\dagger} \sigma_m^{-}$, into the system Hamiltonian.^{18,28} The efficiency of transfer (quantum yield) is then defined as the total probability that the excitation is trapped, $\eta = \sum_m \int_0^{\infty} \kappa_m \langle m | \rho(t) | m \rangle dt$, where $|m\rangle = \sigma_m^+ |0\rangle$.

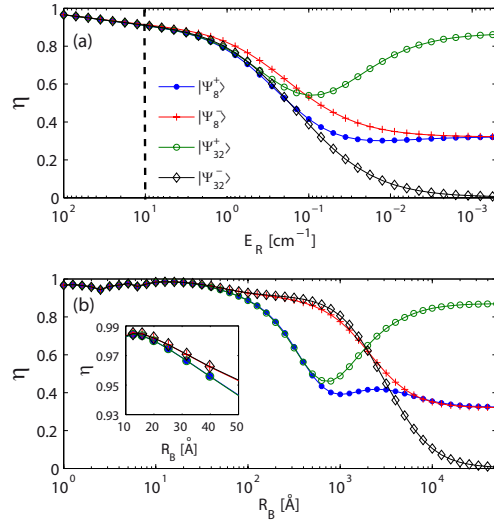


Figure 2: Transfer efficiency at room temperature (293 K): (a) versus on-site reorganization energy E_R in the absence of correlated dephasing. E_R increases from right to left along the horizontal axis to allow easier comparison with below; (b) versus R_B for $E_R = 100 \text{ cm}^{-1}$.

Results - In the following, we assume that all sites dissipate at a rate $\Gamma = 1 \text{ ns}^{-1}$,²⁹ with the exception of the special pair at the RC, which traps excitation at a rate $\kappa = 4 \text{ ps}^{-1}$.²⁹ For LH complexes the system-bath interaction is usually characterized by an Ohmic spectral density with either Drude²⁴ or exponential cutoff;⁹ we assume a Drude form, $\mathcal{J}(\omega) = 2E_R \omega_c \omega / \pi(\omega_c^2 + \omega^2)$. Typical E_R values are estimated to be between 100 cm^{-1} ³⁰ and 200 cm^{-1} ³¹ for LH1, while the bath cutoff frequencies ω_c used to reproduce experimental data range from 50 cm^{-1} ³⁰ to 1000 cm^{-1} .²⁴ Here,

to be consistent with our weak system-bath coupling model and to unambiguously illustrate how initial state distinguishability can arise through spatial correlations, we consider a fast-modulated bath with $\omega_c = 300 \text{ cm}^{-1}$, and a maximum $E_R = 100 \text{ cm}^{-1}$. The ring sites are numbered from 1 to 32 (see [figure][1][1]) and we assume pure initial states, having no overlap with the RC, of the form $|\Psi_m^\pm\rangle = (1/\sqrt{m})\sum_{j=1}^m(\pm 1)^j|j\rangle$, where $1 \leq m \leq 32$. The initial state is thus symmetrically or asymmetrically delocalized over the ring. In particular, we focus on four representative states $|\Psi_8^+\rangle$, $|\Psi_8^-\rangle$, $|\Psi_{32}^+\rangle$, and $|\Psi_{32}^-\rangle$, which in the case of pure coherent evolution ($R_B \rightarrow \infty$ or $E_R = 0$) have, in general, different transfer efficiencies.¹⁸ Further, $|\Psi_{32}^-\rangle$ ($|\Psi_{32}^+\rangle$) has a large degree of overlap with the lowest (highest) eigenstate of H_S . Since the dynamics of ρ varies with respect to pigment-exchange, the results presented correspond to an average over all initial states with delocalization over m consecutive sites.

In [figure][2][2(a)], we plot the transfer efficiency, η , for each initial state as a function of the system-bath coupling quantified by E_R , and accounting only for local dephasing, i.e. $\gamma_{mn}(\omega) = 0$ for $m \neq n$. For small E_R , η varies significantly between the different initial states, consistent with the coherent limit.¹⁸ As E_R increases, exciton relaxation and dephasing take place and above $E_R \gtrsim 10 \text{ cm}^{-1}$ (dashed line), the efficiency becomes practically identical for all initial states considered, indicating that energy transfer is dominated by incoherent processes. Notice that $E_R \sim 10 \text{ cm}^{-1}$ is comparable to the electronic interaction between a Bchl in the ring and the special pair in the center.¹⁸ The situation differs for correlated dephasing, as shown in [figure][2][2(b)]. Here we fix $E_R = 100 \text{ cm}^{-1}$, which falls in the ranges of reported values for an LH1,³⁰ and plot η as a function of the bath correlation length R_B . For large enough values of R_B the efficiency distinguishes again the initial state meaning that coherent dynamics is at play. Two key features can be drawn out from the comparison of [figure][2][2(a)] and (b). First, for moderate values of R_B the transfer efficiency clearly separates symmetric from asymmetric states - we shall shortly discuss the role of coherence and correlations in such distinguishability. Second, for an extended system, increasing R_B does *not* generally correspond simply to a renormalized coupling to an effective local environment at each site. This contrasts with the intuition to be gained by considering the two-site problem ($M = 2$).

In this case, we again use $\sum_{m,n} \mathcal{F}_{mn}(\omega, \rho) = 0$ to rewrite the dissipator as $\mathcal{D}(\rho) = \sum_{\omega} \gamma(\omega) [1 - J_0(d/R_B)] \sum_{m=1,2} \mathcal{F}_{mm}(\omega, \rho)$, where d is the inter-site separation. Here, a finite R_B is equivalent to considering each site to be independently coupled to its own local bath, but with an effective reorganization energy $\tilde{E}_R = E_R [1 - J_0(d/R_B)]$.

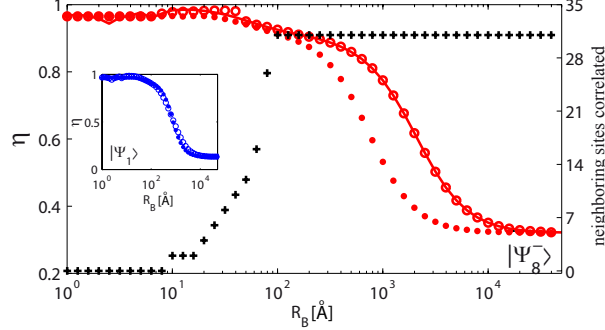


Figure 3: Main: (Left axis) Room temperature transfer efficiency for $|\Psi_8^- \rangle$ against R_B , with $E_R = 100 \text{ cm}^{-1}$: (\bullet) assuming local dephasing with an effective $\tilde{E}_R = E_R [1 - \langle J(d_{mn}/R_B) \rangle]$; (\circ) including only correlations satisfying $J(x) \geq 0.7$; (line) including all correlations. (Right axis) ($+$) Effective number of correlated neighbors to each site. Inset: η versus R_B for the state $|\Psi_1 \rangle$.

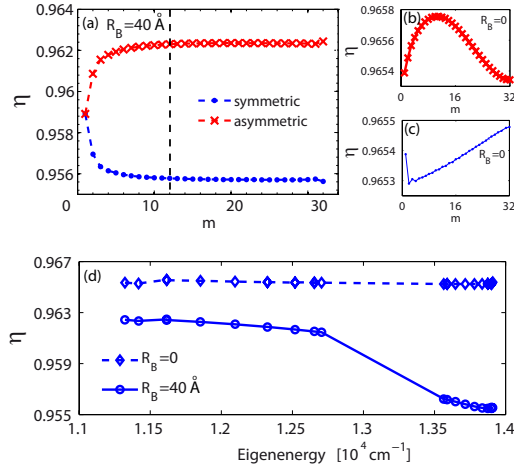


Figure 4: (a) Efficiency for asymmetric and symmetric states as a function of delocalization length m for $R_B = 40 \text{ Å}$. (b-c) show η in the absence of correlations ($R_B = 0$) for asymmetric (b) and symmetric (c) states. (d) Efficiency for eigenstates of H_S having vanishing overlap with the RC for $R_B = 40 \text{ Å}$ (\circ), and $R_B = 0$ (\diamond). In all cases $E_R = 100 \text{ cm}^{-1}$.

Interpretation of the effects of correlated dephasing therefore requires us to go beyond the two-site model. We analyze three different regimes: (i) $R_B < d_{min}$, with $d_{min} \simeq 10 \text{ Å}$ the minimum pair distance in the system; (ii) $R_B \gg d_{max} = 2R$, where $R \simeq 50 \text{ Å}$ is the radius of the ring; and (iii) the

most interesting, intermediate regime $d_{min} < R_B < d_{max}$. In the first two cases the two-site intuition can be applied as fluctuations are only very weakly correlated in case (i), while they are almost completely correlated at all sites in case (ii). In neither case is there significant variation from the average correlation over all $m \neq n$ pairs, $\langle J_0(d_{mn}/R_B) \rangle$. Hence, the dissipator has approximately the same form as the two-site case with an effective reorganization energy $E_R[1 - \langle J_0(d_{mn}/R_B) \rangle]$. This simplified dissipator does not reproduce the transfer efficiency in the intermediate regime for delocalized states, as can be seen in [figure][3][3] where we plot η for the initial state $|\Psi_8^- \rangle$ as an example. Interestingly, for the state $|\Psi_1 \rangle$, which has no quantum superpositions, the effective local-bath approximation captures the efficiency behavior across the whole range of R_B (see [figure][3][3] inset). The key feature, then, is that there is a crucial interplay between coherence, bath correlations, and initial state properties in defining the transfer efficiency. To understand this interplay we can follow an analysis within the quantum jump picture. The system dynamics can be seen as a series of coherent evolutions interrupted by incoherent jumps between single-excitation eigenstates, described by the action of the operator $\gamma_{mn}(\omega)A_m(\omega)\rho(t)A_n^\dagger(\omega)$. In the presence of bath correlations, the overlap with the trapping sites due to such incoherent jumps carries information on the quantum phase differences between sites m and n , through a factor $(\pm 1)^{m+n}$, while in the absence of correlations it does not. Hence, after a jump due to a correlated bath, the subsequent coherent evolution is weighted by a phase factor that is always 1 for symmetric states, but can be 1 or -1 for asymmetric states. This gives rise to the symmetry distinguishability observed in [figure][2][2(b)]. In short, correlated fluctuations promote an *initial state symmetry dependent energy transfer* towards the RC.

Further insight into the behavior of η in the intermediate regime (iii) can be gained by associating R_B to an effective number of neighbors correlated to each site. We estimate this number by neglecting all correlations below a cutoff y ($J_0(d_\alpha/R_B) < y$), chosen to be the largest value that still gives a good agreement with the exact results. For the relevant points in [figure][3][3], we take $y = 0.7$, which corresponds to neglecting all correlations between pairs whose distances satisfy $d_{mn} > 1.1R_B$. In Ref.²⁴ correlations among 5 consecutive sites were included to fit measurements

of optical properties of LH1 samples. From the above analysis, we can associate this number to a correlation length of $R_B \simeq 20 \text{ \AA}$ (see [figure][3][3]). Notice that at this moderate correlation length, η already starts distinguishing states according to their symmetry (inset in [figure][2][2(b)).

With R_B now associated to an effective number of correlated neighbors we are led to conjecture that, for a given R_B , the interplay with coherence will be such that η should increase as a function of the delocalization length (m) for asymmetric states, while it should decrease for symmetric states. Further, such behavior should happen only up to an *optimal delocalization length* m_c , beyond which the efficiency should not considerably change. This is indeed the behavior seen in [figure][4][4(a), where we plot η for asymmetric and symmetric initial states as a function of m , for an intermediate value $R_B = 40 \text{ \AA}$ with associated $m_c \simeq 12$ (dashed line). These results confirm that the interplay of coherence and correlations allows the system to exploit not just asymmetry, but also exciton delocalization. We find, however, that the optimal m_c for which the efficiency plateaus increases only slightly with larger R_B , and is never greater than $m_c \simeq 16$. Hence, m_c is not simply dictated by the length of correlations, but is mainly defined by the symmetry of the electronic interactions in the LH1-RC core. Further, the marked splitting between the two sets of states around the efficiency associated to $m = 1$ clearly illustrates the symmetry-dependent energy transfer discussed above. To highlight the difference to the uncorrelated environments case, [figure][4][4(b-c) show η as a function of m when $R_B = 0$. Importantly, although the variation in η is negligible, its functional form for each set of states is the same as that observed under purely coherent evolution.¹⁸

In the actual light-harvesting process the implications of the above discussed phenomena may be rather subtle. To illustrate this, in [figure][4][4(d) we plot η against energy for all eigenstates having vanishing overlap with the RC. The presence of correlations is manifested in an unexpected ordering of the eigenstates whereby η decreases monotonically with increasing energy. Such order is not observed when correlations vanish. In a functioning photosynthetic system the LH1 donor state will be a thermal distribution about the lowest energy levels.¹⁶ Our results indicate that, without correlations, such a distribution will be as efficient as one about higher states. In contrast,

if correlations are present, a thermal distribution about low-lying states would be the best option. This suggests that the interplay of coherence and correlations could indeed help the natural system to differentiate the best energy transfer pathway.

In summary, we have shown how coherence and bath correlations could equip light-harvesting systems with a mechanism to exploit initial state phase information at room temperature. Although our conclusions are based on a simple model, we conjecture that initial state distinguishability in energy transfer may be a general feature when spatial and/or temporal environmental correlations are present. Hence, experimental explorations of such phenomena could help in elucidating both microscopic details of the environmental correlations as well as the advantages of coherent dynamics in natural and artificial light-harvesting systems.^{4,22}

Acknowledgement

We thank T. Osborne and D. Porras for interesting discussions. F. F. thanks CONICYT for support. A.N and A.O-C acknowledge funding from the EPSRC.

Supporting Information Available

Transfer efficiency at room temperature as a function of R_B including static disorder. It is shown that for $R_B < 2R$, moderate static disorder has no significant effect on the results presented.

This material is available free of charge via the Internet at <http://pubs.acs.org>.

References

- (1) Engel, G. S.; Calhoun, T. R.; Read, E. L.; Ahn, T.-K.; Mančal, T.; Cheng, Y.-C.; Blankenship, R. E.; Fleming, G. R. Evidence for Wavelike Energy Transfer through Quantum Coherence in Photosynthetic Systems. *Nature* **2007**, *446*, 782-786.
- (2) Lee, H.; Cheng, Y.-C.; Fleming, G. R. Coherence Dynamics in Photosynthesis: Protein Protection of Excitonic Coherence. *Science* **2007**, *316*, 1462-1465.

- (3) Collini, E.; Scholes, G. D. Coherent Intrachain Energy Migration in a Conjugated Polymer at Room Temperature. *Science* **2009**, *323*, 369-373.
- (4) Collini, E.; Wong, C. Y.; Wilk, K. E.; Curmi, P. M. G.; Brumer, P.; Scholes, G. D. Coherently Wired Light-Harvesting in Photosynthetic Marine Algae at Ambient Temperature. *Nature* **2010**, *463*, 644-647.
- (5) Scholes, G. D. Quantum-Coherent Electronic Energy Transfer: Did Nature Think of It First? *J. Phys. Chem. Lett.* **2010**, *1*, 2-8.
- (6) Nazir, A. Correlation-Dependent Coherent to Incoherent Transitions in Resonant Energy Transfer Dynamics. *Phys. Rev. Lett.* **2009**, *103*, 146404.
- (7) Beljonne, D.; Curutchet, C.; Scholes, G. D.; Silbey, R. J. Beyond Förster Resonance Energy Transfer in Biological and Nanoscale Systems. *J. Phys. Chem. B* **2009**, *113*, 6583-6599.
- (8) Cheng, Y. C.; Fleming, G. R. Dynamics of Light Harvesting in Photosynthesis. *Annu. Rev. Phys. Chem.* **2009**, *60*, 241-262.
- (9) Renger, T.; May, V. Ultrafast Exciton Motion in Photosynthetic Antenna Systems: The FMO-Complex. *J. Phys. Chem. A* **1998**, *102*, 4381-4391.
- (10) Yu, Z. G.; Berding, M. A.; Wang, H. Spatially Correlated Fluctuations and Coherence Dynamics in Photosynthesis. *Phys. Rev. E* **2008**, *78*, 050902(R).
- (11) Hennebicq, E.; Beljonne, D.; Curutchet, C.; Scholes, G. D.; Silbey, R. J. Shared-Mode Assisted Resonant Energy Transfer in the Weak Coupling Regime. *J. Chem. Phys.* **2009**, *130*, 214505.
- (12) Rebentrost, P.; Mohseni, M.; Aspuru-Guzik, A. Role of Quantum Coherence and Environmental Fluctuations in Chromophoric Energy Transport. *J. Phys. Chem. B* **2009**, *113*, 9942-9947.

- (13) Plenio, M. B.; Huelga, S. F. Dephasing-Assisted Transport: Quantum Networks and Biomolecules. *New J. Phys.* **2008**, *10*, 113019.
- (14) Caruso, F.; Chin, A. W.; Datta, A.; Huelga, S. F.; Plenio, M. B. Highly Efficient Energy Excitation Transfer in Light-Harvesting Complexes: The Fundamental Role of Noise-Assisted Transport. *J. Chem. Phys.* **2009**, *131*, 105106.
- (15) Cheng, Y. C.; Silbey, R. J. Coherence in the B800 Ring of Purple Bacteria LH2. *Phys. Rev. Lett.* **2006**, *96*, 028103.
- (16) Hu, X.; Ritz, T.; Damjanović, A.; Schulten, K. Pigment Organization and Transfer of Electronic Excitation in the Photosynthetic Unit of Purple Bacteria. *J. Phys. Chem. B* **1997**, *101*, 3854-3871.
- (17) Hu, X.; Schulten, K. Model for the Light-Harvesting Complex I (B875) of Rhodospira rubra. *Biophys. J.* **1998**, *75*, 683-694.
- (18) Olaya-Castro, A.; Lee, C.-F.; Fassioli Olsen, F.; Johnson, N. F. Efficiency of Excitation Transfer in Photosynthesis Under Quantum Coherence. *Phys. Rev. B* **2008**, *78*, 085115.
- (19) Damjanović, A.; Ritz, T.; Schulten, K. Excitation Energy Trapping by the Reaction Center of Rhodospira rubra. *Int. J. Quant. Chem.* **2000**, *77*, 139-151.
- (20) Richter, M. F.; Baier, J.; Southall, J.; Cogdell, R. J., Oellerich, S.; Köhler, J. Refinement of the X-ray Structure of the RC-LH1 Core Complex from Rhodospira rubra by Single-Molecule Spectroscopy. *Proc. Nat. Ac. Sci. USA* **2007**, *104*, 20280-20284.
- (21) Scheuring, S. AFM Studies of the Supramolecular Assembly of Bacterial Photosynthetic Core-Complexes. *Curr. Opin. Chem. Biol.* **2006**, *10*, 387-393.
- (22) Womick, J. M.; Miller, S. A.; Moran, A. M. Correlated Exciton Fluctuations in Cylindrical Molecular Aggregates. *J. Phys. Chem. B* **2009**, *113*, 6630-6639.

- (23) Ketelaars, M.; Hofmann, C.; Köhler, J.; Howard, T. D.; Cogdell, R. J.; Schmidt, J.; Aartsma, T. J. Spectroscopy on Individual Light-Harvesting 1 Complexes of Rhodospseudomonas Acidophila. *Biophys. J.* **2002**, *83*, 1701-1715.
- (24) Rutkauskas, D.; Novoderezhkin, V.; Gall, A.; Olsen, J.; Cogdell, R. J.; Hunter, C. N.; van Grondelle, R. Spectral Trends in the Fluorescence of Single Bacterial Light-Harvesting Complexes: Experiments and Modified Redfield Simulations. *Biophys. J.* **2006**, *90*, 2475-2485.
- (25) Olsen, J. D.; Sturgis, J. N.; Westerhuis, W. H. J.; Fowler, G. J. S.; Hunter, C. N.; Robert, B. Site-Directed Modification of the Ligands to the Bacteriochlorophylls of the Light-Harvesting LH1 and LH2 Complexes of Rhodobacter Sphaeroides. *Biochem.* **1997**, *36*, 12625-12632.
- (26) Doll, R.; Wubs, M.; Hänggi, P.; Köhler, S. Limitation of Entanglement due to Spatial Qubit Separation. *EPL* **2006**, *76*, 547-553.
- (27) Breuer, H.-P.; Petruccione, F. *The Theory of Open Quantum Systems*; Oxford University Press: New York, USA, 2002.
- (28) Mohseni, M.; Rebentrost, P.; Lloyd, S.; Aspuru-Guzik, A. Environment-Assisted Quantum Walks in Photosynthetic Energy Transfer. *J. Chem. Phys.* **2008**, *129*, 174106.
- (29) Şener, M.; Schulten, K. Physical Principles of Efficient Excitation Transfer in Light Harvesting, in: *Energy Harvesting Materials*, edited by David L. Andrews, pp. 1-26; World Scientific: Singapore, 2005.
- (30) Renger, T.; Marcus, R. A. On the Relation of Protein Dynamics and Exciton Relaxation in Pigment-Protein Complexes: An Estimation of the Spectral Density and a Theory for the Calculation of Optical Spectra. *J. Chem. Phys.* **2002**, *116*, 9997-10019.
- (31) Freiberg, A.; Rätsep, M.; Timpmann, K.; Trinkunas, G. Excitonic Polarons in Quasi-one-dimensional LH1 and LH2. *Chem. Phys.* **2009**, *357*, 102-112.